ELSEVIER

Journal of Power Sources 111 (2002) 137–144

JOURNAL OF POWER SOURCES

www.elsevier.com/locate/jpowsour

Anodic deposition of nickel oxides for the nickel-based batteries

Chi-Chang Hu*, Chen-Yi Cheng

Department of Chemical Engineering, National Chung Cheng University, Chia-Yi 621, Taiwan

Received 9 October 2001; received in revised form 13 February 2002; accepted 13 May 2002

Abstract

This work represented the preliminary results in developing the anodic deposition of nickel oxides and examining their electrochemical and textural properties for the application in aqueous batteries. Nickel oxides were anodically deposited onto the graphite substrate by cyclic voltammetry (CV) and potentiostatic techniques from the aqueous solution containing $NiCl_2$. Based on the linear sweep voltammogram (LSV) measured from the chloride solution, the anodic deposition of nickel oxides commenced at the onset of the Ni(II)/Ni(III) transition. The electrochemical characteristics, including the specific charge capacity and charge–discharge reversibility, of nickel oxides prepared by the anodic deposition were demonstrated to be the promising electrode materials for nickel-based batteries, which were obviously affected by the potential ranges of CV and the potentials of potentiostatic deposition. The morphologies and crystalline structures of these nickel oxides were respectively examined by scanning electron microscopic photographs and X-ray diffraction (XRD) spectra.

Keywords: Nickel oxide; Anodic deposition; Cyclic voltammetry; Potentiostatic deposition; Nickel-based battery

1. Introduction

As a result of the great practical importance of nickel and nickel-based oxides in a wide range of technological applications, their electrochemical properties in the alkaline media have been widely studied ([1] and references therein). In addition, a model representing the Ni(III)/Ni(II) transition has been established as following:

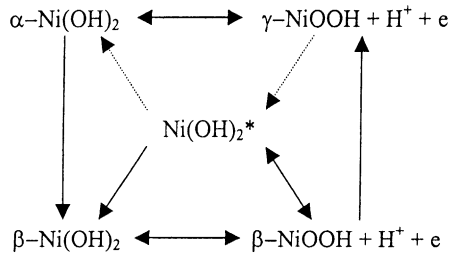

On the other hand, several important steps are still unexplained because of the complicated redox properties of nickel oxides. For example, mechanisms for the irreversible phase transformation from β-NiOOH to γ-NiOOH and from α-$Ni(OH)_2$ to β-$Ni(OH)_2$ are not clearly understood [1]. In addition, the doping of foreign cations (e.g. Co^{2+} and Zn^{2+}) into the nickel oxide matrix was found to improve the utilization of the electroactive material and depress the capacity loss during long charge–discharge cycles [2,3]. However, the actual reasons responsible for this complicated nature of Ni-based oxides in the region of highly positive potentials are still unclear.

Nickel and nickel-based oxides are important electrode materials in nickel-based batteries, which were usually prepared by a sol–gel process or a cathodic precipitation using galvanostatic or potentiostatic methods [2,4–9]. In general, the preparation steps of a sol–gel process are relatively complicated and not easily controlled. It is more desirable to employ the cathodic precipitation to prepare nickel oxides. On the other hand, it is very possible that the cathodically precipitated film is a mixture of metallic nickel and nickel hydroxide, especially in the solutions consisting of chloride precursors [9–11], since metallic Ni is very easily deposited from the cathodic electroplating of free nickel ions. Accordingly, anodic techniques developed for preparing nickel oxides in a wide range of technological applications of batteries, electrochromic devices, water electrolysis, electrosynthesis and fuel cell are considered to be more desirable. Unfortunately, this anodic technique was not often employed for the electrode material preparation [11–13], especially in the application of batteries.

* Corresponding author. Tel.: +886-5-2720411x33411; fax: +886-5-2721206.
E-mail address: chmhcc@ccu.edu.tw (C.-C. Hu).

0378-7753/02/$ – see front matter
PII: S0378-7753(02)00296-3

In this work, anodic deposition processes by means of a potentiostatic technique or cyclic voltammetry (CV) were developed to fabricate nickel oxides. These oxides were deposited from $NiCl_2$ to illustrate powerful features of the anodic deposition in preparing metal oxides since the electroplating of metal oxides from chloride precursors was recognized as a difficult issue ([11] and references therein). The electrochemical reversibility and specific capacity of the Ni(III)/Ni(II) transition on all nickel oxides were systematically investigated using CV and chronopotentiometry (CP) in the alkaline medium for the application of nickel-based batteries. The morphologies and crystalline structures of these materials were examined by scanning electron microscope (SEM) and X-ray diffraction (XRD) technique.

2. Experimental

The 10 mm × 10 mm × 3 mm graphite supports (Nippon Carbon EG-NPL, N.C.K., Japan) were first abraded with ultrafine SiC paper, degreased with acetone and water, then, etched in a 0.1 M HCl solution at room temperature (ca. 26 °C) for 10 min, and finally degreased with water in an ultrasonic bath for 10 min. The exposed geometric area of these pretreated graphite supports is equal to 1 cm^2 while the other surface areas were insulated with polytetrafluorene ethylene (PTFE) coatings. Nickel oxides were directly deposited onto the supports by means of CV in different potential ranges for 60 cycles or by the potentiostatic method in different time periods (i.e. 2300, 4600, 6900 and 9200 s) in a solution containing 0.01 M $NiCl_2$ (Alfa) with initial pH of 8. Note that the scan rate of CV for oxide deposition was equal to 50 mV s^{-1}. The deposition time for the oxide deposits prepared by CV in the potential range of −0.15 to 1.0, 0.3–1.0 and 0.7–1.0 V was equal to 2760, 1680 and 720 s, respectively. Also note that the deposition time for the samples (prepared by the potentiostatic method) with their electrochemical and textural characteristics shown in this work was kept constant (i.e. 4600 s). Since this study is the preliminary work to illustrate the feasibility of anodic deposition and to investigate the basic characteristics of nickel oxide prepared from nickel chloride, a relatively low concentration of electroactive species in the deposition solution was employed here, which may be not high enough for the commercial manufacture. The effect of $NiCl_2$ concentration and other deposition variables (e.g. temperature, pH, loading, intercalation of Co^{2+} and Zn^{2+}, etc.) on the performance of nickel oxide will be carried out in the next work. After deposition, the PTFE films were removed from the electrodes, which were then doubly degreased with pure water and then dried in a vacuum oven at room temperature overnight. The average oxide loading of every oxide-coated electrode is the mean weight difference of an electrode with five measurements without PTFE coating between before and after the application of oxide deposition through a microbalance with an accuracy of 2×10^{-5} g (Sartorius BP 211D, Germany). For the electrochemical studies, the electrode areas without the nickel oxide coatings were doubly coated with epoxy resin and PTFE films while for textural analysis, the electrodes were employed without further treatments.

Surface morphologies of these nickel oxide-coated electrodes were examined by a SEM (JEOL JSM 35). The crystalline information of nickel oxides prepared under different conditions was obtained by XRD patterns (Rigaku X-ray diffractometer using a Cu target) at a scan rate of 4 min^{-1}.

The electrochemical analyzer system, CHI 633A (CH Instruments, USA) was used throughout. Electrochemical and electroplating experiments were carried out in a three-compartment cell. An Ag/AgCl electrode (Argenthal, 3 M KCl, 0.207 V versus SHE at 25 °C) was used as the reference while a platinum wire was employed as the counter electrode. A Luggin capillary, whose tip was set at a distance of 1–2 mm from the surface of the working electrode, was used to minimize errors due to an *iR* drop in the electrolytes.

All solutions used in this work were prepared with pure water produced by a reagent water system (MILLI-Q SP, Japan) at 18 MΩ cm and all reagents not specified in this work are Merck, GR. The solutions used to deposit nickel oxides or to investigate their electrochemical characteristics were degassed with purified nitrogen gas before measurements and a nitrogen blanket was used during the measurements. The solution temperature was maintained at 25 °C by means of a water thermostat (HAAKE DC3 and K20).

3. Results and discussion

The potential range of anodic deposition of nickel oxide can be reasonably estimated from the *i–E* curve of the nickel chloride oxidation in the deposition bath [11]. A typical linear sweep voltammogram (LSV) measured in a 0.01 M $NiCl_2$ solution with pH of 8.0 at 25 °C is shown in Fig. 1a. On this curve, there is a passive response at potentials negative to 0.6 V, indicating the inhibition of Ni(II) oxidation since the Ni(III)/Ni(II) transition should commence at ca. 0.35 V (versus Ag/AgCl). This effect is attributable to the energy barrier for the anodic deposition of the nickelous precursor because of the chloride coordination. Note the broad anodic peak between 0.6 and 1.0 V, which is attributed to the oxidation and conversion of $NiCl_2$ to nickel oxide. Accordingly, the anodic deposition of nickel oxides is expected to occur between 0.6 and 1.0 V. Also note the sharp increase in anodic currents at potentials positive than 1.1 V, which is due to the oxygen evolution reaction.

Based on the earlier results and discussion, nickel oxide may be anodically deposited onto graphite substrates from the above plating bath at potentials between 0.6 and 1.0 V. Typical results of the oxide loading against the deposition time for the oxides deposited at 0.7, 0.8 and 0.9 V are shown in Fig. 1b. Note that for the oxide deposited at 0.7 V, the loading is gradually increased with increasing the deposition

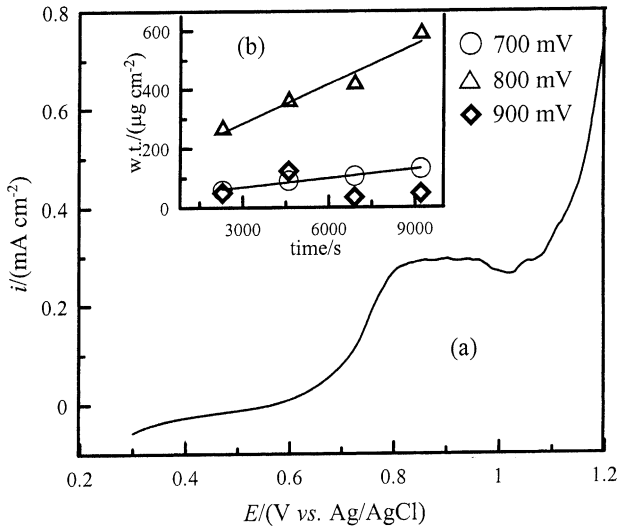

Fig. 1. (a) A LSV measured in a 0.01 M $NiCl_2$ solution with pH of 8.0 at 25 °C. (b) The dependence of loading against the deposition time for the nickel oxide deposited at 0.7, 0.8 and 0.9 V.

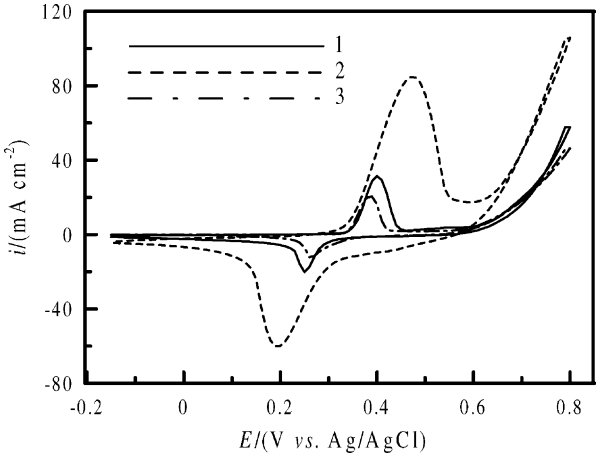

Fig. 2. Cyclic voltammograms measured at 25 mV s^{-1} in 1 M NaOH for the nickel oxide deposited at (1) 0.7 V, (2) 0.8 V and (3) 0.9 V.

time meanwhile the loading is increased more quickly with increasing the deposition time for the oxide deposited at 0.8 V. However, the dependence of oxide loading on the deposition time is irregular when the oxide is deposited at 0.9 V. In fact, the rate of oxide deposition should be increased with increasing the overpotential of deposition. However, this newly deposited oxide is collapsed and many black particles are dispersed in the plating solution during the anodic deposition. This result is attributable to the poor adhesion of the nickel oxide prepared at this potential and/or the repulsive force of oxygen bubbles since visible bubbles are found on the oxide surface. On the other hand, the increase in the weight of the graphite support after the anodic polarization in a 0.01 M $NiCl_2$ solution does indicate the fact that nickel oxide can be anodically deposited onto an inert substrate from its chloride precursor.

In order to gain further electrochemical information of the nickel oxide deposits prepared by the potentiostatic method, the voltammetric behavior of these oxide-coated electrodes was examined through CV in NaOH. Typical CV curves, measured at 25 mV s^{-1} in 1 M NaOH, for the nickel oxides deposited at 0.7, 0.8 and 0.9 V are shown as curves 1–3, respectively in Fig. 2. From a comparison of the *i*–*E* curves in Fig. 2 with those of nickel oxides prepared by the cathodic precipitation or sol–gel techniques [2,4–9], these three CV curves show the intrinsically electrochemical features of nickel oxide. (i) Passive behavior is found at potentials negative to 0.32 V and an anodic peak attributed to the oxidation of Ni(II) to Ni(III) is clearly found on the positive sweep at potentials of 0.32–0.42, 0.32–0.53 and 0.32–0.41 V for curves 1–3, respectively. (ii) The sharp increase in anodic currents on both positive and negative sweeps at potentials positive than ca. 0.6 V indicates oxygen evolution reaction. (iii) The corresponding reduction peaks of Ni(III) are obviously found on the negative sweeps. Note that the voltammetric charges of both peaks are proportional to their loading, indicating that the redox transition of electroactive nickel species within the whole deposit can proceed in a similar potential range. Also note that the oxidation of electroactive nickel species shows the bell-shape anodic peak on the positive sweeps and its corresponding reduction on the negative sweeps shows a cathodic peak in a similar shape (in the opposite direction). In addition, the voltammetric charge of the cathodic peak is approximately equal to that of its corresponding anodic peak. Thus, the anodic peak is said to be symmetric in shape to its corresponding cathodic peak, indicating the good electrochemical reversibility (i.e. the charge–discharge efficiency should be high) although their peak potentials on the positive and negative sweeps are not equal. Therefore, these oxides are considered to be the suitable electrode materials for nickel-based batteries. On the other hand, the peak potential difference (ΔE_p) for this pair of redox peaks increases with the oxide loading, suggesting that the reversibility as well as the charge–discharge efficiency of nickel oxide should be significantly affected by their loading and/or thickness.

From the LSV behavior of $NiCl_2$ oxidation, nickel oxide should be able to be deposited by means of CV, although this method seems to be more complicated than that of a potentiostatic method. In addition, it is very possible that the newly deposited nickel species move on the oxide surface to the energy-favorable sites during the passive region (i.e. at potentials negative to 0.6 V) on both positive and negative sweeps [14]. Thus, the electrochemical properties (e.g. reversibility and specific capacity) of nickel oxides prepared by CV may be different from that fabricated by the potentiostatic method. Based on this point of view, three deposits were electroplated by CV for 60 cycles at 50 mV s^{-1} from −0.15 to 1.0, 0.3–1.0 and 0.7–1.0 V, respectively. Their CV curves measured at 25 mV s^{-1} in 1 M NaOH are shown in Fig. 3 as curves 1–3, respectively, where their loading is 6.4×10^{-5}, 10.2×10^{-5} and 8.4×10^{-5} g, respectively. From an examination of these

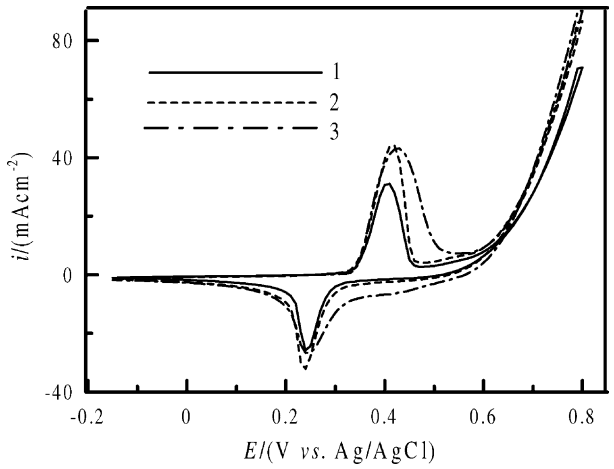

Fig. 3. Cyclic voltammograms measured at 25 mV s^{-1} in 1 M NaOH for the nickel oxide deposited by CV at 50 mV s^{-1} in the potential region of (1) −0.15 to 1.0 V, (2) 0.3–1.0 V and (3) 0.7–1.0 V.

CV curves in Fig. 3, the voltammetric behavior of these electrodes also shows the typical *i–E* responses of nickel oxide. However, the voltammetric charges corresponding to the redox transition of Ni(III)/Ni(II) are not proportional to their loading, indicating that the specific capacity of nickel oxides prepared by CV is significantly affected by the potential region of oxide deposition. Note that the peak potential difference (ΔE_p) for this pair of redox peaks is approximately independent of the loading or voltammetric charge of the oxides and the anodic peak is very symmetric to its cathodic peak (i.e. CV curves are similar in shape and their voltammetric charges are approximately equal) on these curves. The earlier results indicate a good reversibility of the Ni(III)/Ni(II) couple for the nickel oxides prepared by CV, which are considered as the suitable electrode materials for nickel-based batteries.

There should exist so-called ''inner'' and ''outer'' active surface areas on the oxide-coated electrodes fabricated in this work since all electroactive nickel species within the oxide matrix involve the redox transition in a similar potential range. In addition, the oxidation and reduction of Ni(III)/Ni(II) involve the exchange of proton or OH^-. This effect may delay the redox transition due to the diffusion of ions within the oxide film, which have been proposed to be distinguishable by studying the dependence of $1/q^*$ on the square root of scan rate of CV ($v^{1/2}$) [15]. Accordingly, the voltammetric charges (i.e. q^*) of these nickel oxide deposits were integrated from the negative sweeps of CVs measured at different scan rates and in different-pH solutions with constant ionic strength. The results of the dependence of $1/q^*$ on $v^{1/2}$ obtained in 1 M NaOH, 0.1 M NaOH + 0.3 M Na_2SO_4 and 0.01 M NaOH + 0.33 M Na_2SO_4 are shown in Fig. 4a–c. In order to circumvent the effect of pH on the potential region of the Ni(III)/Ni(II) transition, the potential region of CV in this study is located between 0.90 and 1.65 V against the reversible hydrogen electrode (RHE). Note that for the same electrode, the slope of $1/q^*$ against

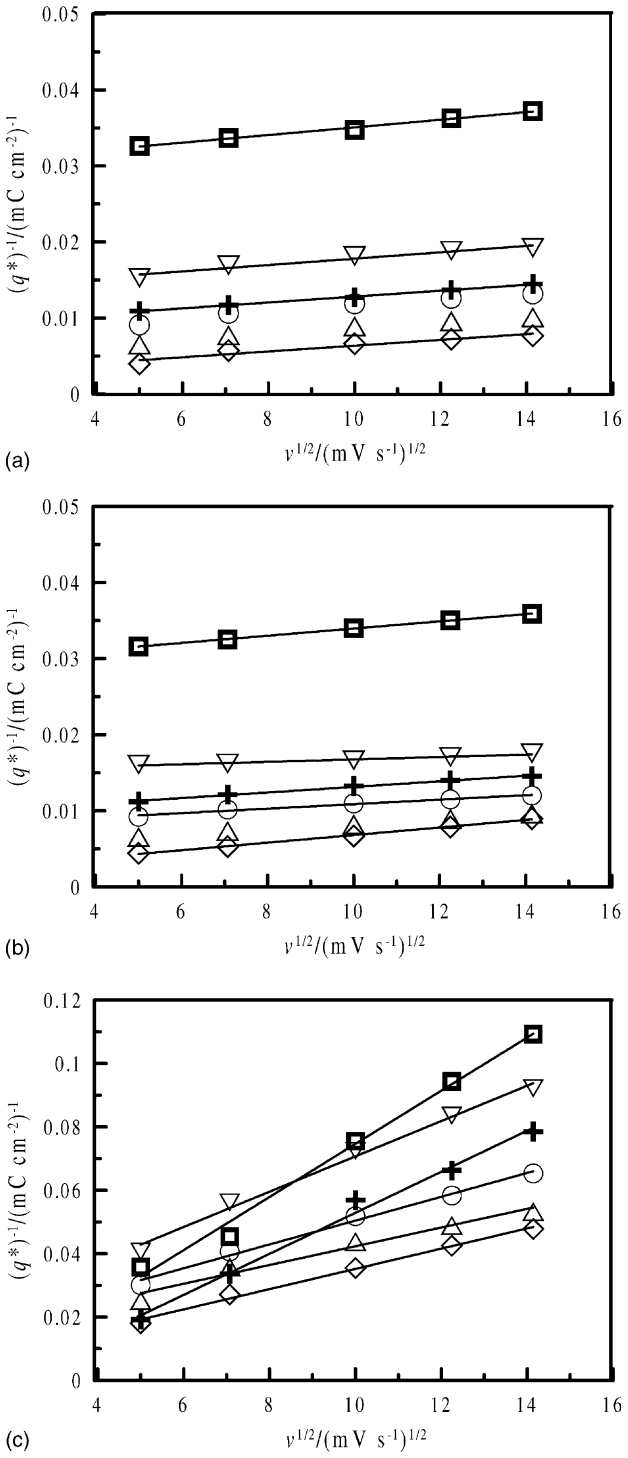

Fig. 4. Dependence of $1/q^*$ on $v^{1/2}$, where q^* was the cathodic charge of the negative sweep on a cyclic voltammogram measured at 25 °C in (a) 1 M NaOH, (b) 0.1 M NaOH + 0.3 M Na_2SO_4 and (c) 0.01 M NaOH + 0.33 M Na_2SO_4. The nickel oxides were prepared by: CV in the potential range of (○) −0.15 to 1.0 V, (△) 0.3–1.0 V and (▽) 0.7–1.0 V; the potentiostatic method at (✚) 0.7 V, (◇) 0.8 V and (◘) 0.9 V.

$v^{1/2}$ is approximately constant when the concentration of OH^- is higher than 0.1 M. However, an obvious increase is found when the concentration of OH^- is below 0.1 M although the sequence of electrodes with respective to

increasing the slope is irregular. The earlier results imply that OH^- should be the exchange ion during the redox transition and that the ''inner'' active surface area within these nickel oxide deposits is absent when the concentration of OH^- is higher than 0.1 M. Hence, most electroactive nickel species can freely proceed the Ni(III)/Ni(II) transition in a concentrated OH^- solution. The Ni(III)/Ni(II) transition is thus considered to exhibit a good electrochemical reversibility on these nickel oxide deposits in concentrated alkaline solutions.

The inference that OH^- should be the exchange ion during the redox transition of Ni(III)/Ni(II) is further confirmed by examining the redox behavior of nickel oxide in the electrolytes with different pH. Typical CV results for the nickel oxide electrode deposited by CV between 0.3 and 1.0 V measured in 1 M NaOH, 0.1 M NaOH + 0.3 M Na_2SO_4 and 0.01 M NaOH + 0.33 M Na_2SO_4 are shown as curves 1–3 in Fig. 5. Note that the redox peaks become wider when the OH^- concentration is changed from 1.0 to 0.1 M. In addition, the voltammetric currents and charges of Ni(III)/Ni(II) couples are obviously decreased when the OH^- concentration is decreased to 0.01 M, indicating the loss of active sites for the energy storage. The earlier effects are likely due to the lower concentration gradient for the OH^- diffusion during the process of Ni(III)/Ni(II) transition in an electrolyte with a lower concentration of OH^-. If proton is the exchange species during the Ni(III)/Ni(II) transition, the voltammetric currents corresponding to the Ni(III)/Ni(II) couple should be increased with increasing the concentration of proton. However, an opposite result is found. Based on the earlier result and discussion, OH^- is more reasonably attributed to the exchange ion during the redox transition of Ni(II)/Ni(III). Also note that the peak potentials of the Ni(III)/Ni(II) couple are not significantly affected by the change in pH of the test electrolytes. This result indicates that the ratio of the electron-transfer number and OH^- exchange number is equal to 1 since these CV diagrams are shown in the RHE scale.

The charge–discharge behavior of the earlier mentioned nickel oxides was also examined in 1 M NaOH solution. Typical results for the charge and discharge curves obtained at 2 C are shown in Fig. 6a and b, respectively. In Fig. 6a, all the curves show a plateau between 0.33 and 0.39 V and a corresponding plateau between 0.30 and 0.26 V is found during the discharge process (see Fig. 6b). The mean potential difference of the two plateaus is about 80 mV, indicating a fair reversibility of the Ni(III)/Ni(II) transition. It is worth noting that the specific capacity (based on the discharge capacity in milliampere hour per gram) of nickel oxides prepared by potential cycling is obviously higher than that prepared by the potentiostatic method. In addition, the specific capacity of the nickel oxide with the largest loading (i.e. prepared at 0.8 V) is obviously smaller than that of the others. The former result indicates that the electrochemical properties of nickel oxide prepared by the anodic methods are expected to be strongly dependent upon the preparation techniques. The latter result suggests that the specific capacity of nickel oxide is significantly influenced by its thickness and/or structure that is a function of the preparation

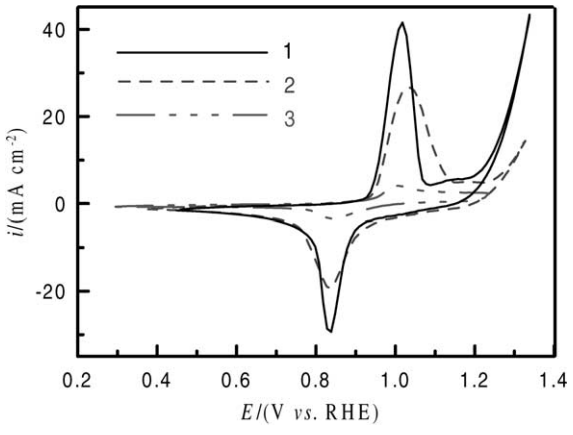

Fig. 5. Cyclic voltammograms measured at 25 mV s^{-1} in (1) 1 M NaOH, (2) 0.1 M NaOH + 0.3 M Na_2SO_4 and (3) 0.01 M NaOH + 0.33 M Na_2SO_4 for the nickel oxide deposited by CV at 50 mV s^{-1} in the potential region of 0.3–1.0 V.

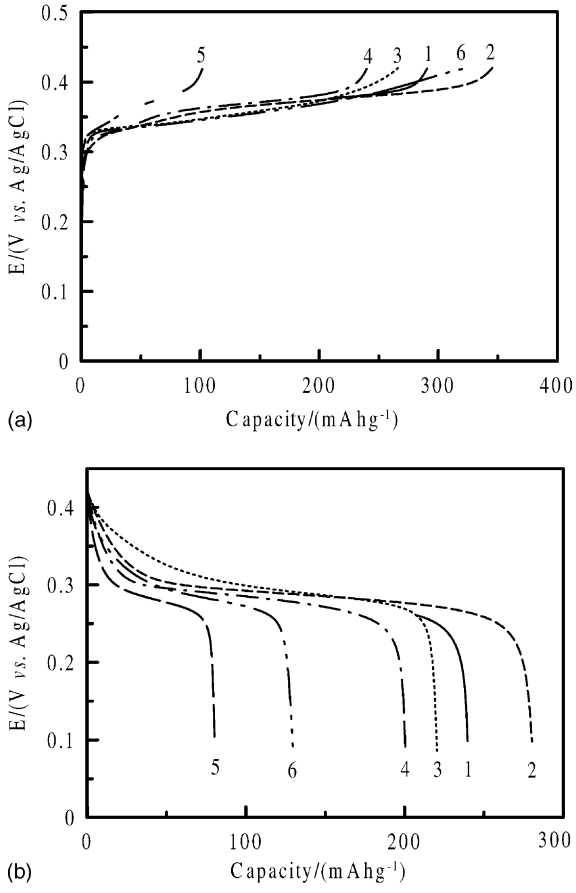

Fig. 6. (a) Charge and (b) discharge curves at 2 C in 1 M NaOH for the nickel oxides prepared by: CV in the potential range of (1) −0.15 to 1.0 V, (2) 0.3–1.0 V and (3) 0.7–1.0 V; the potentiostatic method at (4) 0.7 V, (5) 0.8 V and (6) 0.9 V.

methods and conditions. Also note the largest difference in specific capacity between the charge and discharge curves for the nickel oxide prepared at 0.9 V (i.e. see curve 6 in Fig. 6a and b), indicating the significant irreversibility of the Ni(III)/Ni(II) transition on this oxide. All the earlier differences in both specific capacity and the reversibility are attributable to a combination of the following reasons. First, the electrochemical methods as well as the potential ranges of the electrode preparation should result in the change in structures for nickel oxide since the structure of nickel oxides was found to strongly depend on the oxidation state of nickel [16,17]. In addition, nickel oxides with different structures were found to exhibit different specific capacities [18]. Thus, the reversibility of the Ni(III)/Ni(II) transition should be strongly dependent on the electrochemical methods and the potential ranges for plating the nickel oxide deposit. Unfortunately, for all nickel oxide deposits prepared in this work, there is no diffraction peak corresponding to nickel oxides in any phases on their XRD patterns (Fig. 9). Thus, the difference in structures for these oxide deposits cannot be exactly pointed out in this work. Second, the diffusion length of OH^- during the charge–discharge test is longer for the thicker deposits. The specific capacity of a thicker deposit should be lower under a relatively high charge–discharge current density (e.g. 2 and 4 C in our case), resulting in the lowest specific capacity of the nickel oxide with the largest loading.

Fig. 7 shows the specific capacity, measured at 4 C during the discharge process, of various nickel oxides prepared by the anodic deposition against the number of charge–discharge curves. In general, the specific capacity of these oxides decreases with the number of charge–discharge curves. In addition, the decrease in specific capacity for all oxides is quicker during the first four to seven runs. In our opinion, the nickel oxides prepared in this work can be

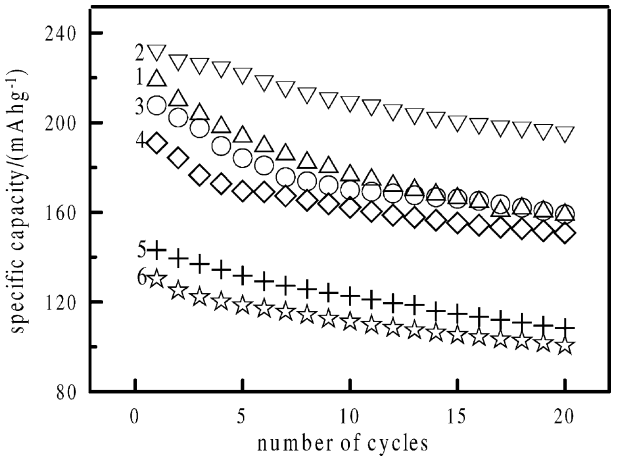

Fig. 7. Dependence of the specific capacity obtained from the discharging curve at 4 C on the number of charge–discharge curves for the nickel oxides prepared by: CV in the potential range of (1) −0.15 to 1.0 V, (2) 0.3–1.0 V and (3) 0.7–1.0 V; the potentiostatic method at (4) 0.7 V, (5) 0.8 V and (6) 0.9 V.

considered as an aggregate consisting of Ni^{2+}, Ni^{3+}, OH^-, H_2O and other cations (e.g. NH_4^+) with a non-stoichiometric nature [12,18–20]. The arrangement of the nickel oxides should not be well organized and ordered, especially under a higher rate of deposition (e.g. the potentiostatic deposition at 800 and 900 mV). This speculation is supported by the amorphous nature of these deposits (see the XRD patterns in Fig. 9). If this is the case, many defects (e.g. sites of oxygen deficiency, nickel deficiency, etc.) should be formed within these nickel oxide deposits. Since the structure as well as the volume of nickel oxides will be gradually changed with varying the electric energy stored in the oxides [16–18,21,22], a rearrangement in the structure for the nickel aggregates during the charge–discharge test should occur. This rearrangement probably results in the decrease of defects and a decrease in specific capacity for these oxide deposits is obviously found during the first four to seven runs of the charge–discharge tests. Thus, the charge–discharge process is believed to provide the energy to overcome the energy barrier of oxide rearrangement. On the basis of the earlier results and discussion, the specific capacity decreases very slowly and approximately steadily after the first few runs of charge–discharge. The earlier proposal is also supported by the fact that the capacity of the charge process becomes equal to that of the discharge process when the first few runs of charge–discharge have been carried out.

For the nickel oxide prepared by the chemical precipitation in a hot spraying process, its maximum capacity is about 260 mAh g^{-1} while its discharge current density is only about 1/2 C [18]. For the nickel oxide prepared by the chemical precipitation process, its maximum capacity is about 180 mAh g^{-1} under the 1/12.5 C discharge density [21]. In our work, the nickel oxide deposited via the anodic process possesses the maximum capacity of ca. 280 and 235 mAh g^{-1} under the 2 and 4 C discharge current densities, respectively, which is 96.9 and 81.3% utilization of the electroactive material, respectively. The maximum capacity of the nickel oxide prepared in this work is approximately equal to that prepared by the chemical precipitation in a hot spraying process although the capacity of the other nickel oxide deposits prepared in this work is not always as high as that of the hot spraying process. Moreover, the step of our work is simpler in comparison with that of the hot spraying process and the capacity of nickel oxide is strongly dependent upon the charge–discharge current density. Based on the earlier comparison, the nickel oxides prepared in this work are concluded to be potential materials for the nickel-based batteries.

Typical scanning electron microscopic photographs of the nickel oxide deposits prepared by CV during the −0.15 to 1.0, 0.3–1.0, and 0.7–1.0 V and by the potentiostatic method at 0.7, 0.8 and 0.9 V are shown in Fig. 8. In fact, the surface morphology of the graphite substrate is relatively rough and porous [23]. This rough and porous surface can be completely covered with the oxide films by the above two anodic techniques since all deposits show a porous and/or cracked

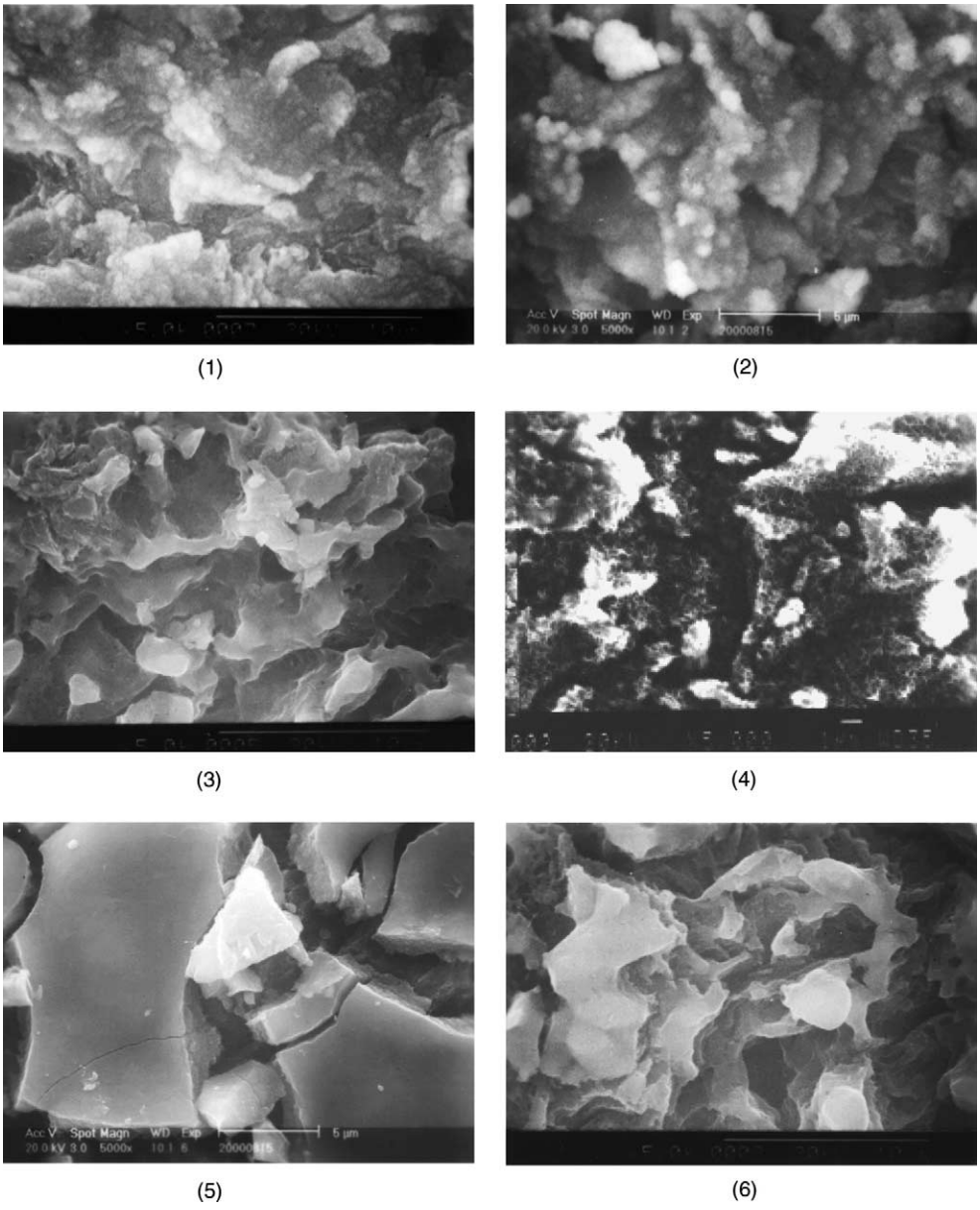

Fig. 8. Scanning electron microscopic photographs of the nickel oxides prepared by: CV in the potential range of (1) −0.15 to 1.0 V, (2) 0.3–1.0 V and (3) 0.7–1.0 V; the potentiostatic method at (4) 0.7 V, (5) 0.8 V and (6) 0.9 V.

nature which is very different from that of a porous graphite substrate. Note that the morphologies of the nickel oxide grains prepared by CV with its lower potential limit (E_{SC}) negative to 0.3 V are in general spherical (Fig. 8(1) and (2)). The presence of obvious spherical grains of nickel oxides further supports the proposal that the newly deposited nickel species should move on the oxide surface to the energy-favorable sites during the passive region on both positive and negative sweeps. The spherical morphology, however, is changed to an irregular and porous morphology when E_{SC} is changed to 0.7 V (Fig. 8(3)). In Fig. 8(4), the morphology of nickel oxide is very rough and porous while some large pores/cracks distributed on the deposit, which can be attributable to the porous nature of the graphite substrate. In Fig. 8(5), a relatively compact and mud-cracked morphology is found on this deposit. In Fig. 8(6), a very porous and irregular morphology is clearly found, which may result from the significant collapse of this deposit during the anodic deposition. All the earlier results reveal the fact that the morphologies of nickel oxides are significantly affected by the techniques and conditions of anodic deposition.

Since the morphologies of the nickel oxides mentioned earlier are functions of deposition techniques and conditions, their structures may be also affected by these variables, resulting in the difference in specific capacity. Moreover, nickel oxides prepared by the cathodic precipitation showed a crystalline structure and exhibited suitable electrochemical properties for nickel-based batteries [3,7].

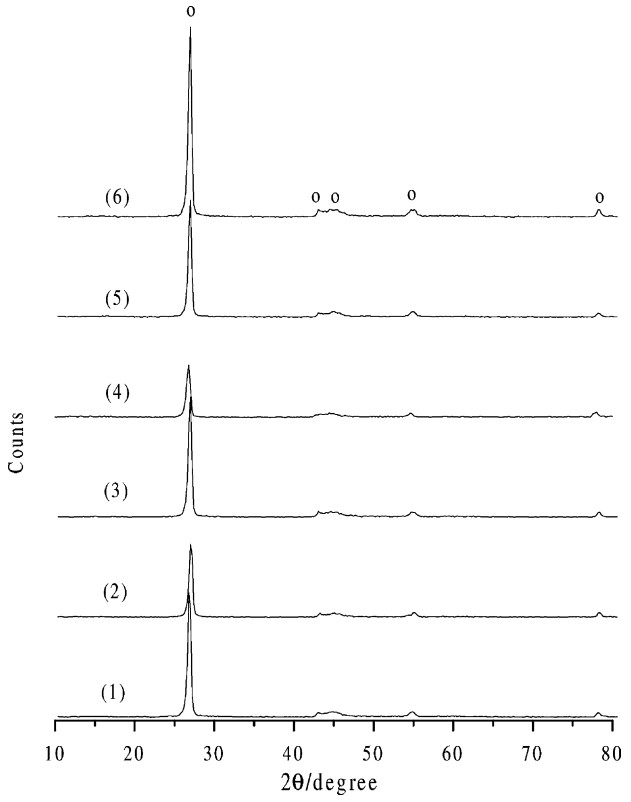

Fig. 9. XRD patterns of the nickel oxides prepared by: CV in the potential range of (1) −0.15 to 1.0 V, (2) 0.3–1.0 V and (3) 0.7–1.0 V; the potentiostatic method at (4) 0.7 V, (5) 0.8 V and (6) 0.9 V.

Thus, the crystalline information for these deposits prepared through the anodic methods is examined. Typical XRD patterns for the nickel oxide films prepared by CV during the −0.15 to 1.0, 0.3–1.0, and 0.7–1.0 V and by the potentiostatic method at 0.7, 0.8 and 0.9 V are shown as curves 1–6, respectively, in Fig. 9. Note that there are only diffraction peaks of graphite (labeled as o) on these spectra. The earlier result indicates two facts. First, the absence of diffraction peaks corresponding to nickel oxide indicates that nickel oxides prepared through means of the anodically potentiostatic and CV techniques have an amorphous structure that is different from the case prepared by the cathodic precipitation [3,7]. This result supports the proposal that the nickel oxides prepared in this work can be considered as an aggregate consisting of Ni^{2+}, Ni^{3+}, OH^-, H_2O and other cations with a non-stoichiometric nature [12,18–20]. Second, the presence of graphite diffraction peaks indicates the thin-film nature of nickel oxides prepared by the anodic deposition methods.

4. Conclusions

The anodic deposition of nickel oxide occurred during the Ni(II)/Ni(III) transition. Nickel oxides anodically deposited by CV and potentiostatic techniques from the chloride precursor solution were demonstrated to be a promising material for the nickel-based batteries. The electrochemical reversibility of Ni(III)/Ni(II) couple for all deposits was examined by CV, which was obviously affected by the OH^- concentration of the examination solutions. The specific capacity of nickel oxides prepared by CV was significantly higher than that prepared by the potentiostatic method, which was also affected by the potential ranges of CV and the potentials of the potentiostatic deposition. The morphologies of nickel oxides prepared by the anodic deposition showed a rough nature, which were very different from that of the porous graphite substrate. The XRD patterns revealed that all nickel oxides prepared in this work exhibited an amorphous structure.

Acknowledgements

The financial support of this work, by the National Science Council of the Republic of China under contract no. NSC 90-2214-E-194-007, is gratefully acknowledged.

References

[1] T.-C. Wen, C.-C. Hu, Y.-J. Li, J. Electrochem. Soc. 140 (1993) 2554.
[2] B.B. Ezhov, O.G. Malandin, J. Electrochem. Soc. 138 (1991) 885.
[3] M.E. Unates, M.E. Folquer, J.R. Vilche, A.J. Arvia, J. Electrochem. Soc. 139 (1992) 2697.
[4] D.F. Pickett, J.T. Maloy, J. Electrochem. Soc. 125 (1978) 1026.
[5] M.E. Folquer, J.R. Vilche, A.J. Arvia, J. Electrochem. Soc. 127 (1980) 2634.
[6] Y. Mo, E. Hwang, D.A. Scherson, J. Electrochem. Soc. 143 (1996) 37.
[7] I. Serebrennikova, V.I. Birss, J. Electrochem. Soc. 144 (1997) 566.
[8] M.-S. Kim, T.-S. Hwang, K.-B. Kim, J. Electrochem. Soc. 144 (1997) 1537.
[9] Y. Sasaki, T. Yamashita, Thin Solid Films 334 (1998) 117.
[10] M. Pourbaix, Atlas of Electrochemical Equilibria in Aqueous Solutions, Pergamon Press, Oxford, 1966.
[11] G.H.A. Therese, P.V. Kamath, Chem. Mater. 12 (2000) 1195.
[12] Y.-W.D. Chen, R.N. Noufi, J. Electrochem. Soc. 131 (1984) 1447.
[13] M.-C. Yang, C.-K. Lin, C.-L. Su, J. Electrochem. Soc. 142 (1995) 1189.
[14] C.-C. Hu, K.-Y. Liu, Electrochim. Acta 44 (1999) 2727.
[15] S. Ardizzone, G. Fregonara, S. Trasatti, Electrochim. Acta 35 (1990) 263.
[16] H. Bode, K. Dehmelt, J. Witte, Electrochim. Acta 11 (1966) 1079.
[17] D. Singh, J. Electrochem. Soc. 145 (1998) 116.
[18] J. Chen, D.H. Bradhurst, S.X. Dou, H.K. Liu, J. Electrochem. Soc. 146 (1999) 3606.
[19] M. Dixit, P.V. Kamath, J. Gopalakrishnan, J. Electrochem. Soc. 146 (1999) 79.
[20] C.-C. Hu, C.-Y. Chen, Electrochem. Solid Sate Lett. 5 (2002) A43.
[21] M.B.J.G. Freitas, J. Power Sources 93 (2001) 163.
[22] P. Elumalai, H.N. Vasan, N. Munichandraiah, J. Power Sources 93 (2001) 201.
[23] C.-C. Hu, C.-H. Chu, J. Electroanal. Chem. 503 (1/2) (2001) 105.